3400 *Chem. Mater.* **2009,** *21,* 3400–3405
DOI:10.1021/cm901008t

CHEMISTRY OF MATERIALS
Article

Structural Properties of Multiferroic $BiFeO_3$ under Hydrostatic Pressure

Alexei A. Belik,*[,†] Hitoshi Yusa,[‡] Naohisa Hirao,[§] Yasuo Ohishi,[§] and Eiji Takayama-Muromachi[†]

[†]*International Center for Materials Nanoarchitectonics (MANA) and* [‡]*Advanced Nano Materials Laboratory (ANML), National Institute for Materials Science (NIMS), 1-1 Namiki, Tsukuba, Ibaraki 305-0044, Japan, and* [§]*Synchrotron Radiation Research Institute (JASRI), 1-1-1 Kouto, Sayo-cho, 679-5198, Hyogo, Japan*

Received April 13, 2009

High-pressure structural properties of multiferroic perovskite-type $BiFeO_3$ have been investigated by high-resolution synchrotron X-ray powder diffraction at room temperature up to 9.7 GPa. $BiFeO_3$ shows rather complicated structural behavior. The ambient-pressure ferroelectric $R3c$ phase transforms to an orthorhombic phase OI at around 4 GPa during compression. The OI phase is characterized by a superstructure $\sqrt{2}a_p \times 3\sqrt{2}a_p \times a_p$, where a_p is the parameter of the cubic perovskite subcell ($a = 5.4939(4)$ Å, $b = 16.6896(9)$ Å, $c = 3.8728(2)$ Å at 4.9 GPa). The OI phase transforms to an orthorhombic phase OII at around 7 GPa. The OII phase is characterized by a superstructure $\sqrt{2}a_p \times 3\sqrt{2}a_p \times 2a_p$ ($a = 5.5021(3)$ Å, $b = 16.2439(11)$ Å, $c = 7.6960(4)$ Å at 9.7 GPa). During decompression, significant hysteretic behavior was found. The OII phase was stable down to about 3 GPa. The OII phase then transforms to an orthorhombic phase OIII that is characterized by a superstructure $\sqrt{2}a_p \times 2\sqrt{2}a_p \times 2a_p$ ($a = 5.5617(6)$ Å, $b = 11.2153(10)$ Å, $c = 7.7788(7)$ Å at 2.2 GPa). The $R3c$ phase appeared below about 1 GPa; however, even at ambient pressure, traces of the OIII phase remained. The OIII phase seems to be isostructural with antiferroelectric $PbZrO_3$ (space group *Pbam*).

1. Introduction

$BiFeO_3$ is a perovskite-type oxide crystallizing in space group $R3c$ with $a_H = 5.579$ Å and $c_H = 13.869$ Å (in hexagonal setting) at room temperature (RT) and ambient pressure (AP).[1] $BiFeO_3$ is a unique material.[2] First, it is the only compound among simple $BiMO_3$ systems (M = transition metals) that can be prepared at AP in bulk form. (Note that with multiple M ions, some other materials with only Bi^{3+} ions occupying the A site in ABO_3 perovskite can also be prepared at ambient pressure, e.g., $Bi_2Mn_{4/3}Ni_{2/3}O_6$ and $Bi_2Ti_{3/8}Fe_{2/8}Mg_{3/8}O_6$).[3,4] Second, $BiFeO_3$ is a very rare example of a single-phase RT multiferroic.[2,5] In multiferroic systems, two or all three of (anti)ferroelectricity, (anti)ferromagnetism, and ferroelasticity are observed in the same phase.[6,7] In $BiFeO_3$, the ferroelectric Curie temperature $T_E = 1100$ K and antiferromagnetic Néel temperature $T_N = 640$ K are both well above RT; and $BiFeO_3$ is ferroelastic.[2] Third, it shows a very large spontaneous polarization[8] and very interesting low-temperature[9−11] and high-temperature behavior.[12−18] There are several high-temperature modifications of $BiFeO_3$ whose symmetry and structures are still a matter of debate in the literature.[12−18] Possible reasons of discrepancy are discussed in ref 19; it is also possible that differences in stoichiometry play an important role.

*To whom correspondence should be addressed. E-mail: Alexei.Belik@nims.go.jp.

(1) Kubel, F.; Schmid, H. *Acta Crystallogr., Sect. B* **1990**, *46*, 698.
(2) Wang, J.; Neaton, J. B.; Zheng, H.; Nagarajan, V.; Ogale, S. B.; Liu, B.; Viehland, D.; Vaithyanathan, V.; Schlom, D. G.; Waghmare, U. V.; Spaldin, N. A.; Rabe, K. M.; Wuttig, M.; Ramesh, R. *Science* **2003**, *299*, 1719.
(3) Hughes, H.; Allix, M. M. B.; Bridges, C. A.; Claridge, J. B.; Kuang, X.; Niu, H.; Taylor, S.; Song, W.; Rosseinsky, M. J. *J. Am. Chem. Soc.* **2005**, *127*, 13790.
(4) Bridges, C. A.; Allix, M.; Suchomel, M. R.; Kuang, X. J.; Sterianou, I.; Sinclair, D. C.; Rosseinsky, M. J. *Angew. Chem., Int. Ed.* **2007**, *46*, 8785.
(5) Ramesh, R.; Spaldin, N. A. *Nat. Mater.* **2007**, *6*, 21.
(6) Hill, N. A. *J. Phys. Chem. B* **2000**, *104*, 6694.
(7) Eerenstein, W.; Mathur, N. D.; Scott, J. F. *Nature* **2006**, *442*, 759.
(8) Neaton, J. B.; Ederer, C.; Waghmare, U. V.; Spaldin, N. A.; Rabe, K. M. *Phys. Rev. B* **2005**, *71*, 014113.
(9) Singh, M. K.; Katiyar, R. S.; Prellier, W.; Scott, J. F. *J. Phys.: Condens. Matter* **2009**, *21*, 042202.
(10) Redfern, S. A. T.; Wang, C.; Hong, J. W.; Catalan, G.; Scott, J. F. *J. Phys.: Condens. Matter* **2008**, *20*, 452205.
(11) Singh, M. K.; Prellier, W.; Singh, M. P.; Katiyar, R. S.; Scott, J. F. *Phys. Rev. B* **2008**, *77*, 144403.
(12) (a) Kornev, I. A.; Lisenkov, S.; Haumont, R.; Dkhil, B.; Bellaiche, L. *Phys. Rev. Lett.* **2007**, *99*, 227602. (b) Gonzalez-Vazquez, O. E.; Iniguez, J. *Phys. Rev. B* **2009**, *79*, 064102.
(13) Valant, M.; Axelsson, A. K.; Alford, N. *Chem. Mater.* **2007**, *19*, 5431.
(14) Scott, J. F.; Palai, R.; Kumar, A.; Singh, M. K.; Murari, N. M.; Karan, N. K.; Katiyar, R. S. *J. Am. Ceram. Soc.* **2008**, *91*, 1762.
(15) Palai, R.; Katiyar, R. S.; Schmid, H.; Tissot, P.; Clark, S. J.; Robertson, J.; Redfern, S. A.; Catalan, G.; Scott, J. F *Phys. Rev. B* **2008**, *77*, 014110.
(16) Selbach, S. M.; Tybell, T.; Einarsrud, M. A.; Grande, T. *Adv. Mater.* **2008**, *20*, 3692.
(17) Selbach, S. M.; Einarsrud, M. A.; Grande, T. *Chem. Mater.* **2009**, *21*, 169.
(18) Arnold, D. C.; Knight, K. S.; Morrison, F. D.; Lightfoot, P. *Phys. Rev. Lett.* **2009**, *102*, 027602.
(19) Redfern, S. A. T.; Walsh, J. N.; Clark, S. M.; Catalan, G.; Scott J. F. **2009**, arXiv:0901.3748v2.

Published on Web 06/12/2009

Table 1. Pressure Dependence of Lattice Parameters in $BiFeO_3$ during Compression up to 9.7 GPa and Decompression

pressure (GPa)	a (Å)	b (Å)	c (Å)	V (Å^3), Z	system
AP up	5.5814(1)		13.8718(4)	374.25(2), 6	*R*3*c*
0.8 up	5.5684(2)		13.7939(5)	370.41(2), 6	*R*3*c*
1.8 up	5.5560(1)		13.7317(4)	367.10(2), 6	*R*3*c*
3.4 up	5.5394(2)		13.6399(6)	362.46(2), 6	*R*3*c*
4.9 up	5.4939(4)	16.6896(9)	3.8728(2)	355.10(4), 6	*Cmmm*, OI
5.9 up	5.4737(3)	16.6504(8)	3.8636(2)	352.12(3), 6	*Cmmm*, OI
7.5 up	5.4548(6)	16.595(2)	3.8539(4)	348.87(7), 6	*Cmmm*, OI, ∼65%
	5.5328(15)	16.313(4)	7.7237(17)	697.1(3), 12	*Ibam*, OII, ∼35%
8.7 up	5.5130(3)	16.2873(10)	7.7014(4)	691.57(7), 12	*Ibam*, OII
9.7 up	5.5021(3)	16.2439(11)	7.6960(4)	687.84(7), 12	*Ibam*, OII
5.4 down	5.5452(4)	16.4237(11)	7.7516(4)	705.97(8), 12	*Ibam*, OII
3.7 down	5.5658(5)	16.5151(15)	7.7712(6)	714.32(10), 12	*Ibam*, OII
2.2 down	5.5617(6)	11.2153(10)	7.7788(7)	485.21(8), 8	*Pbam*, OIII
0.9 down	5.5959(3)	11.2500(6)	7.7899(4)	490.41(4), 8	*Pbam*, OIII, ∼70%
	5.5696(4)		13.7801(13)	370.20(5), 6	*R*3*c*, ∼30%

Dozens or even hundreds of papers have already been published on $BiFeO_3$. However, $BiFeO_3$ continues to attract a lot of attention. One of the recent topics on $BiFeO_3$ is its structural, electronic, and magnetic properties under high pressure (HP).[19−25] HP behavior of a material is important for understanding its properties, instabilities, and design of new functions like in the case of ferroelectric $BaTiO_3$ and $PbTiO_3$.[26] One group has reported (based on synchrotron X-ray powder diffraction (SXRD)) that there are no structural changes in $BiFeO_3$ up to very high pressure of 70 GPa at RT.[22,23] Another group has found two structural phase transitions under HP at 3 and 7 GPa by Raman and infrared spectroscopy[21,24,25] and at 3.6−4 and 10−12 GPa by SXRD.[25] The *R*3*c* phase is stable between AP and 3 GPa; a monoclinic *C*2/*m* phase was reported to exist between 3 and 9 GPa;[25] and a $GdFeO_3$-type phase (space group *Pnma*) was found between 12 and 37 GPa.[25] The appearance of the $GdFeO_3$-type phase is in agreement with the first-principle calculations.[20] There is clear evidence that the $GdFeO_3$-type phase is stable above 10−12 GPa (for example, the observation of the typical (111) reflection for $GdFeO_3$-type phases).[19,25] However, structural properties of $BiFeO_3$ below 10 GPa are not well clarified.

In this work, we investigated structural properties of $BiFeO_3$ at RT up to 9.7 GPa during compression and decompression. We found at least three new orthorhombic phases of $BiFeO_3$. During compression, the phase transitions take place at about 4 and 7 GPa in agreement with the infrared spectroscopy measurements.[24,25] During decompression, a large hysteresis was found. A phase isostructural with antiferroelectric $PbZrO_3$ was found in the vicinity of the ferroelectric *R*3*c* phase.

2. Experimental Section

Synthesis of $BiFeO_3$. A stoichiometric mixture of Bi_2O_3 (99.99%) and Fe_2O_3 (99.9%) was placed in Au capsules and treated at 6 GPa in a belt-type high-pressure apparatus at 1273 K for 30 min. After heat treatment the sample was quenched to RT, and the pressure was slowly released. X-ray powder diffraction (XRD) showed that the sample contained small amount of $Bi_2O_2CO_3$, $Bi_{25}FeO_{39}$, and Fe_2O_3 as impurities.

Synchrotron X-ray Powder Diffraction (SXRD) Experiments at High Pressure. A symmetric diamond anvil cell (DAC), equipped with a culet diameter of 0.4 mm, was used for the high-pressure experiments. The powder $BiFeO_3$ sample was put into a chamber (0.15 mm in diameter) in a rhenium gasket (0.8 mm in thickness) with a few small grains of ruby (less than 5 μm) to measure pressure.[27] The sample was immersed in a pressure medium (methanol:ethanol:water = 16:3:1) to present a hydrostatic condition. The in situ XRD experiments were performed at RT on BL04B2 at SPring-8.[28] A monochromatic X-ray beam (38 keV) was focused and collimated to the sample within 50 μm size. Diffracted X-rays were detected by an imaging plate (IP). The distance from the IP to the sample was kept as long as possible (L = 640.060) in the X-ray diffractometer so that a high-energy X-ray (λ = 0.3278 Å) could be used to get an accurate value for d. Typical exposure time was 20 min. Diffraction patterns were collected with increasing pressure up to 9.7 GPa at intervals of 1−2 GPa. After that, the patterns in decompression process were taken. After each compression or decompression step, the DAC was left for at least 1 h to reduce the pressure fluctuations prior to taking the SXRD pattern. In the studied pressure range, the hydrostaticity was completely kept because no freezing of the pressure medium was observed under optical microscope. Diffraction data were analyzed by the Rietveld method with RIETAN-2000.[29]

3. Results and Discussion

Between AP and 3.4 GPa on compression, we clearly observed the *R*3*c* phase even though the rhombohedral

(20) Ravindran, P.; Vidya, R.; Kjekshus, A.; Fjellvag, H.; Eriksson, O. *Phys. Rev. B* **2006**, *74*, 224412.
(21) Haumont, R.; Kreisel, J.; Bouvier, P. *Phase Transitions* **2006**, *79*, 1043.
(22) Gavriliuk, A. G.; Struzhkin, V. V.; Lyubutin, I. S.; Troyan, I. A. *JETP Lett*. **2007**, *86*, 197.
(23) Gavriliuk, A. G.; Struzhkin, V. V.; Lyubutin, I. S.; Ovchinnikov, S. G.; Hu, M. Y.; Chow, P. *Phys. Rev. B* **2008**, *77*, 155112.
(24) Pashkin, A.; Rabia, K.; Frank, S.; Kuntscher, C. A.; Haumont, R.; Saint-Martin, R.; Kreisel, J. **2007**, arXiv:0712.0736v1.
(25) Haumont, R.; Bouvier, P.; Pashkin, A.; Rabia, K.; Frank, S.; Dkhil, B.; Crichton, W. A.; Kuntscher, C. A.; Kreisel, J. **2008**, arXiv:0811.0047v1 and *Phys. Rev. B* **2009**, 79, 184110.
(26) (a) Wu, Z. G.; Cohen, R. E. *Phys. Rev. Lett*. **2005**, *95*, 037601. (b) Ahart, M.; Somayazulu, M.; Cohen, R. E.; Ganesh, P.; Dera, P.; Mao, H. K.; Hemley, R. J.; Ren, Y.; Liermann, P.; Wu, Z. G. *Nature (London)* **2008**, *451*, 545.
(27) Mao, H. K.; Xu, J.; Bell, P. M. *J. Geophys. Res*. **1986**, *91*, 4673–4676.
(28) Kohara, S.; Itou, M.; Suzuya, K.; Inamura, Y.; Sakurai, Y.; Ohishi, Y.; Takata, M. *J. Phys.: Condens. Matter* **2007**, *19*, 506101.
(29) Izumi, F.; Ikeda, T. *Mater. Sci. Forum* **2000**, *321−324*, 198.

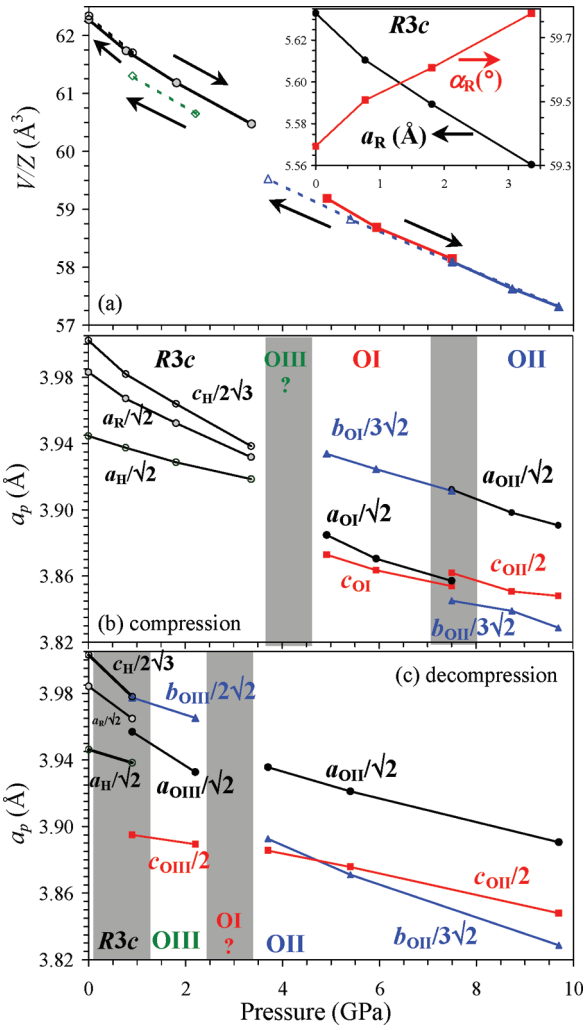

Figure 1. (a) Pressure dependence of unit-cell volume V divided by Z (Z is the number of formula units per unit cell) in $BiFeO_3$ at room temperature during increase in pressure (solid lines) and decrease in pressure (broken lines). Inset shows the pressure dependence of the lattice parameters of the $R3c$ phase (in rhombohedral setting a_R and α_R) on compression. (b) Pressure dependence of the normalized (to the cubic perovskite a_p) lattice parameters on compression. (c) Pressure dependence of the normalized lattice parameters on decompression. Grey rectangles show the two-phase regions. Errors along y-axes are smaller than the symbols. For the $R3c$ phase, the lattice parameters in hexagonal setting a_H and c_H and a_R are shown.

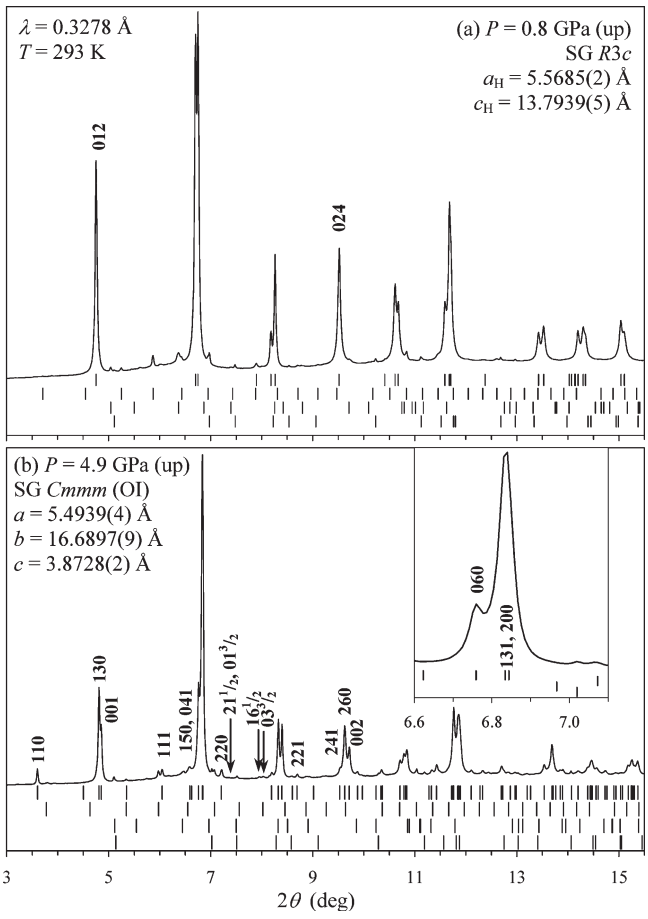

Figure 2. Synchrotron X-ray powder diffraction patterns of $BiFeO_3$ at room temperature and at (a) 0.8 and (b) 4.9 GPa on compression. The allowed Bragg reflections for the corresponding space groups are indicated by tick marks. The refined lattice parameters and indices of some reflections are given. The Bragg reflections are shown for a perovskite phase, $Bi_{25}FeO_{39}$, $Bi_2O_2CO_3$, and Fe_2O_3, respectively, from top to bottom.

distortion and peak splitting decreased with pressure, as can be seen from approaching the rhombohedral angle α_R to the ideal value of 60° for the cubic modification (see Table 1, the inset of Figure 1, and Figure 2a).

At 4.9 GPa on compression, the crystal symmetry was obviously different (Figure 2b). The hexagonal (012) and (024) reflections split clearly. In addition, a lot of weak superstructure reflections appeared. The main subcell and main superstructure reflections could be indexed in an orthorhombic system characterized by a superstructure $\sqrt{2}a_p \times 3\sqrt{2}a_p \times a_p$, where a_p is the parameter of the cubic perovskite subcell. This modification will be called OI. The observed reflection conditions afford the maximum space group *Cmmm*.[30] We note that we observed a few very weak reflections that require the doubled c axis for the indexing (Figure 2b) (the maximum space group with the doubled c axis is *Immm*). However, for the purpose of clarity, we kept the $\sqrt{2}a_p \times 3\sqrt{2}a_p \times a_p$ superstructure (Table 1).

At 7.5 GPa on compression, the orthorhombic $(110)_{OI}$ reflection was clearly split indicating the existence of a mixture of two phases (Figure 3). A new modification between 7.5 and 9.7 GPa will be called OII. Above 7.5 GPa, the pressure behavior of the $(110)_{OII}$ reflection was different compared with the behavior of the $(110)_{OI}$ reflection between 4.9 and 7.5 GPa. The main subcell and main superstructure reflections of the OII phase could be indexed in an orthorhombic system characterized by a superstructure $\sqrt{2}a_p \times 3\sqrt{2}a_p \times 2a_p$. The observed reflection conditions afford the maximum space group *Ibam*.[30] We emphasize that doubling of the c axis was necessary in this case because of the presence of rather strong $(211)_{OII}$ superstructure reflection (see Figure 4a).

Therefore, our SXRD data confirmed the HP structural phase transitions at around 3.5−4 and 7 GPa (during compression) in agreement with the results of infrared spectroscopy studies.[24,25] There is noticeable volume

(30) Hahn, T. International Tables for Crystallography, 5th; ed. Kluwer: Dordrecht, The Netherlands, 2002; Vol. A, p 52.

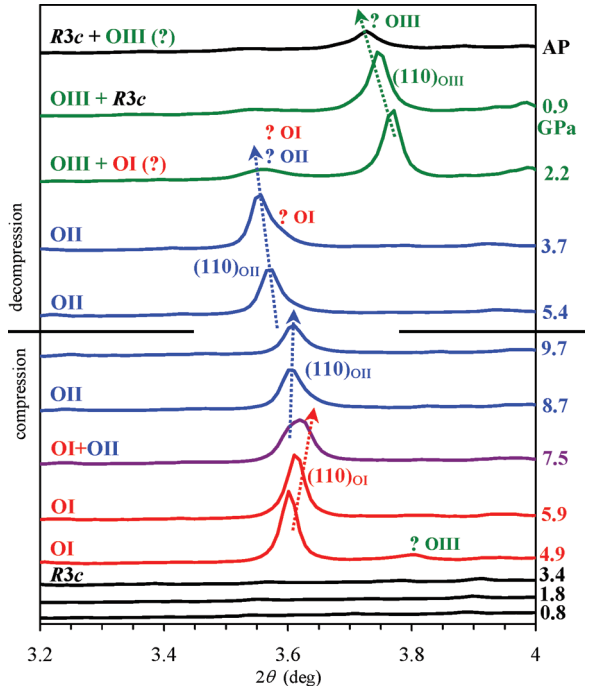

Figure 3. Fragment (from 3.2 to 4° in 2θ) of synchrotron X-ray powder diffraction patterns of $BiFeO_3$ at room temperature on compression and decompression, emphasizing the evolution of superstructure reflections. At 2.2 GPa, weak peaks near 3.55 and 4.00° can also be due to the doubled c axis.

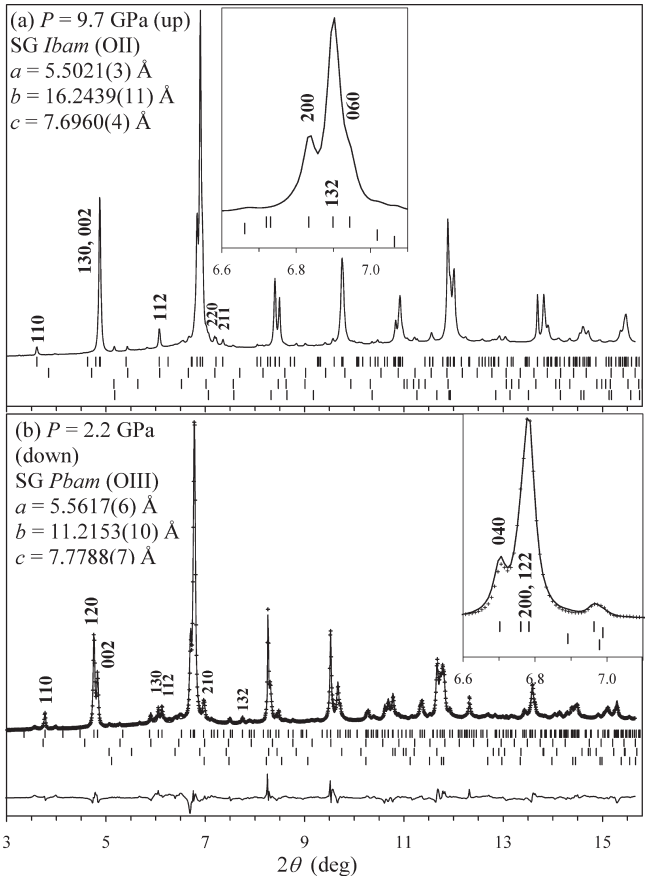

Figure 4. Synchrotron X-ray powder diffraction patterns of $BiFeO_3$ at room temperature and at (a) 9.7 GPa (on compression) and (b) 2.2 GPa (on decompression). The allowed Bragg reflections for the corresponding space groups are indicated by tick marks. The refined lattice parameters and indices of some reflections are given. The Bragg reflections are shown for a perovskite phase, $Bi_{25}FeO_{39}$, $Bi_2O_2CO_3$, and Fe_2O_3, respectively, from top to bottom. In (b), the observed, calculated, and difference SXRD patterns are shown.

drop during the $R3c \Rightarrow$ OI transition (Figure 1a) typical for a first-order phase transition; however, the volume change during the OI $\Rightarrow$ OII transition is very small. Nevertheless, the normalized (to the cubic perovskite a_p) lattice parameters showed steplike changes during the OI $\Rightarrow$ OII transition indicating the first-order phase transition (Figure 1b). Above 10−12 GPa, the OII $\Rightarrow$ *Pnma*($GdFeO_3$-type) transition takes place; the *Pnma* phase is characterized by a superstructure $\sqrt{2}a_p \times 2a_p \times \sqrt{2}a_p$ and has the characteristic (111) reflection.[25]

In ref 25, a monoclinic system (space group $C2/m$; a_M = 17.5218 Å, b_M = 7.7244 Å, c_M = 5.4711 Å, and β_M = 108.24 at 6.2 GPa) was reported between 4 and 10 GPa (on compression); that is, the OI and OII phases were not resolved. Our SXRD patterns at 4.9 and 5.9 GPa could be well-fitted with the given $C2/m$ model (see the Supporting Information). However, at 8.7 and 9.7 GPa, this model could not fit all superstructure reflections (for example, the $(110)_{OII}$ reflection). The relationship between the $C2/m$ cell and our orthorhombic cell is $a_{OI} = c_M$, $b_{OI} = a_M\sin(\beta_M)$, $c_{OI} = 0.5b_M$. It is possible that at 6.2 GPa two phases OI and OII already coexisted in ref 25 or the OI phase is polar; this is why the monoclinic system was necessary to describe all observed reflections. We also note that the reported $C2/m$ structural model is a very rough approximation because the calculated Bi−O bond lengths vary between 1.8 and 3.0 Å, and the Fe−O bond lengths between 1.3 and 2.8 Å.

On decompression from 9.7 GPa, the OII phase existed down to 3.7 GPa (Figures 1c and 3). At 3.7 GPa, a shoulder from the right side appeared on the $(110)_{OII}$ reflection. This shoulder may indicate the appearance of traces of the OI phase. However, at 2.2 GPa on decompression, a new superstructure appeared (Figure 3). This new modification will be called OIII (it has two characteristic superstructure reflections (130) and (112) (Figure 4b)). The main subcell and main superstructure reflections of the OIII phase could be indexed in an orthorhombic system characterized by a superstructure $\sqrt{2}a_p \times 2\sqrt{2}a_p \times 2a_p$. The observed reflection conditions afford the maximum space group *Pbam*.[30] The superstructure and space group of the OIII phase have analogues among the perovskite-type compounds; namely, antiferroelectric $PbZrO_3$ has the same space group and superstructure.[31] Therefore, we used structural data of $PbZrO_3$ as the indicial ones in the Rietveld fitting. We refined only lattice parameters and fractional coordinates of Bi and Fe fixing all thermal parameters and fractional coordinates for oxygen atoms. Even this constrained model gave rather good matching between the observed and calculated SXRD patterns (Figure 4b). This fact shows that the OIII phase should be isostructural with antiferroelectric $PbZrO_3$. At 2.2 GPa, traces of the OI or

(31) Glazer, A. M.; Roleder, K.; Dec, J. *Acta Crystallogr., Sect. B* **1993**, *49*, 846.

OII phases or the 2*c* superstructure may exist (Figure 3). There is noticeable volume increase during the OII⇒OIII and OIII⇒*R*3*c* transitions on decompression (Figure 1a) indicating first-order phase transitions.

At 0.9 GPa on decompression, a mixture of two phases was observed: the OIII phase (about 70 wt %) and the *R*3*c* phase (about 30 wt %). At AP after pressing, a few extra reflections remained on the SXRD pattern (Figure 3 and the Supporting Information), probably due to the stress effect.

Therefore, our results showed rather complicated structural behavior of $BiFeO_3$ under pressure at RT. A large hysteretic behavior was also found. Even we could not observe the OIII phase during compression it is possible that it may appear in a very narrow pressure range between 3.4 and 4.9 GPa (Figure 3). Similarly, the phase I may appear during decompression in a very narrow pressure range between 3.7 and 2.2 GPa. It is possible that these phases may not be observed as single phase but as a mixture with adjacent phases. Our results coupled with the literature data[19,24,25] suggest the following sequence of the phase transitions on compression: *R*3*c* ⇒ OIII(?) ⇒ OI ⇒ OII ⇒ *Pnma*($GdFeO_3$-type) ⇒ cubic. The appearance of the (antiferroelectric) OIII phase near the ferroelectric *R*3*c* phase is very interesting because this fact shows instabilities of $BiFeO_3$ under pressure. On the other hand, the ferroelectric *R*3*c* phase is very stable at AP and transforms directly to the paraelectric *Pnma* phase.[18]

The *Pnma* phase was also found in $BiMO_3$ (M = Sc (above 3.7 GPa), Cr (above 1.0 GPa), Mn (above 6.0 GPa), and Ni (above 4.0 GPa)) at RT.[32,33] The high-temperature and HP phases of $BiCrO_3$ and $BiMnO_3$ can be stabilized at ambient conditions by different substitutions. For example, isovalent substitutions in the Mn sublattice of $BiMnO_3$ ($BiMn_{1-x}M_xO_3$ with M = Al, Sc, Cr, Fe, and Ga and $0 \le x \le 0.2$) stabilize the high-temperature phase II of $BiMnO_3$.[34] The introduction of cation vacancies ($BiMnO_{3+\delta}$ (δ = 0.08 and 0.12) or $Bi_{1-y}Mn_{1-y}O_3$)[35] stabilizes the high-pressure P-phase of $BiMnO_3$.[33] And isovalent substitutions in the Bi sublattice of $BiMnO_3$ (and $BiCrO_3$) ($Bi_{1-x}M_xMnO_3$ with M = Y and La) stabilize the high-temperature or high-pressure *Pnma* phase of $BiMnO_3$.[33] It is known that $Bi_{1-x}M_xFeO_3$ with M = La and Gd crystallizes in space group *Pnma* (corresponding to the HP phase of $BiFeO_3$ above 10 GPa).[36] Quite recently it was found that $Bi_{1-x}Nd_xFeO_3$ with $x = 0.15$ and 0.2 has a structure closely related to that of antiferroelectric $PbZrO_3$,[37] that is, corresponding to the OIII HP phase of $BiFeO_3$. Therefore, stabilization of other HP phases of $BiFeO_3$ by different substitutions is highly possible.

Investigation of properties under high pressure is rather difficult, especially above 4 GPa. Above 4 GPa, one can mainly perform different spectroscopic or diffraction measurements in diamond anvil cells or resistivity measurements. Raman and infrared spectroscopy and X-ray emission spectroscopy studies have already been done at high pressure.[23−25] Resistivity measurements of $BiFeO_3$ have been performed up to 60 GPa.[23] Insulating states preserved up to 40 GPa, and an insulator−metal transition was found between 40 and 50 GPa. Insulating states were also found in $Bi_{0.8}Nd_{0.2}FeO_3$ with the OIII structure[37] and in $Bi_{0.7}Gd_{0.3}FeO_3$ with the *Pnma* structure at ambient pressure.[36] Stabilization of HP phases of $BiFeO_3$ at ambient conditions by different substitutions opens possibilities to investigate other properties that cannot be studied at high pressure.

In refs 22 and 23, it was reported that the rhombohedral phase(s) is stable up to 70 GPa. Even the resolution was not enough to see well the splitting of the main perovskite reflections the superstructure reflections (during compression, decompression, and at AP after pressing) were observed; however, they were not taken into account.[22,23] It is also interesting to note that the SXRD pattern at 68.3 GPa reported in refs 22 and 23 shows splitting of the strongest perovskite reflection. On the other hand, ref 19 reports that the cubic phase appeared at about 45 GPa. Therefore, the stability range of the cubic phase needs further investigation.

For the high-temperature β phase of $BiFeO_3$ above 1100 K, a variety of structural models have recently been proposed: cubic, tetragonal, orthorhombic, monoclinic, and rhombohedral.[12,15−19] The possible reasons are (1) the phase coexistence; (2) high-temperature experiments where it is difficult to control the exact sample temperature; (3) partial sample decomposition, and therefore, changes in the stoichiometry and structural behavior; (4) use of X-ray powder diffraction where it is difficult to locate oxygen atoms.[19] Neutron powder diffraction[18] or single-crystal X-ray diffraction are needed for the careful structural characterization. The same is true for the HP structural behavior. We found different complex superstructures (with weak superstructure reflections and large lattice parameters) and presence of mixtures of different phases. Therefore, the precise determination of space groups and polarity and subsequent structural analysis is possible only using neutron powder diffraction or preferably single-crystal X-ray diffraction. (For this reason, we do not give any structural models in this work even though we used the Rietveld method in the analysis of the SXRD patterns because the obtained models are rough approximations (similar to the *C*2/*m* model in ref 25) except for the OIII phase). We also note that structural behavior on decompression may depend on the maximum applied pressure.

In conclusion, we found three new orthorhombic phases of $BiFeO_3$ at room temperature below 9.7 GPa.

(32) Azuma, M.; Carlsson, S.; Rodgers, J.; Tucker, M. G.; Tsujimoto, M.; Ishiwata, S.; Isoda, S.; Shimakawa, Y.; Takano, M.; Attfield, J. P. *J. Am. Chem. Soc.* **2007**, *129*, 14433.
(33) Belik, A. A.; Yusa, H.; Hirao, N.; Ohishi, Y.; Takayama-Muromachi, E. *Inorg. Chem.* **2009**, *48*, 1000.
(34) Belik, A. A.; Takayama-Muromachi, E. *Inorg. Chem.* **2007**, *46*, 5585.
(35) Belik, A. A.; Kolodiazhnyi, T.; Kosuda, K.; Takayama-Muromachi, E. *J. Mater. Chem.* **2009**, *19*, 1593.
(36) Khomchenko, V. A.; Kiselev, D. A.; Bdikin, I. K.; Shvartsman, V. V.; Borisov, P.; Kleemann, W.; Vieira, J. M.; Kholkin, A. L. *Appl. Phys. Lett.* **2008**, *93*, 262905.
(37) Karimi, S.; Reaney, I. M.; Levin, I.; Sterianou, I. *Appl. Phys. Lett.* **2009**, *94*, 112903.

During compression, the phase transitions take place at about 4 and 7 GPa. On decompression, the phase transitions take place at about 3 and 1 GPa. We found a new phase isostructural with antiferroelectric $PbZrO_3$ in the vicinity of the ferroelectric $R3c$ phase of $BiFeO_3$.

Acknowledgment. This work was supported by World Premier International Research Center (WPI) Initiative on Materials Nanoarchitectonics, MEXT, Japan, and by the NIMS Individual-Type Competitive Research Grant. The synchrotron radiation experiments were performed at SPring-8 with the approval of the Japan Synchrotron Radiation Research Institute

Supporting Information Available: Details of fitting results in the $C2/m$ model and XRD patterns of $BiFeO_3$ at ambient pressure before compression and after decompression (PDF). This material is available free of charge via the Internet at http://pubs.acs.org.